SLAC-PUB-15904

LASER AND PLASMA ACCELERATOR WORKSHOP

Laser Ionized Preformed Plasma at FACET

S.Z. Green[1], E. Adli[1,3], C.I. Clarke[1], S. Corde[1], S.A. Edstrom[1], A.S. Fisher[1], J. Frederico[1], J.C. Frisch[1], S. Gessner[1], S. Gilevich[1], P. Hering[1], M.J. Hogan[1], R.K. Jobe[1], M. Litos[1], J.E. May[1], D.R. Walz[1], V. Yakimenko[1], C.E. Clayton[2], C. Joshi[2], K.A. Marsh[2], N. Vafaei-Najafabadi[2], P. Muggli[4]

[1]SLAC National Accelerator Laboratory, Menlo Park, CA 94025
[2]University of California Los Angeles, 90095
[3]University of Oslo, 0316 Oslo, Norway
[4]Max Planck Institute for Physics, Munich, Germany

E-mail: selina@slac.stanford.edu

Abstract. The Facility for Advanced Accelerator and Experimental Tests (FACET) at SLAC installed a 10-TW Ti:Sapphire laser system for pre-ionized plasma wakefield acceleration experiments. High energy (500 mJ), short (50 fs) pulses of 800-nm laser light at 1 Hz are used at the FACET experimental area to produce a plasma column. The laser pulses are stretched to 250 fs before injection into a vapor cell, where the laser is focused by an axicon lens to form a plasma column that can be sustained over the desired radius and length. A 20-GeV electron bunch interacts with this preformed plasma to generate a non-linear wakefield, thus accelerating a trailing witness bunch with gradients on the order of several GV/m. The experimental setup and the methods for producing the pre-ionized plasma for plasma wakefield acceleration experiments performed at FACET are described.

PACS numbers: 52.59.Bi, 52.59.Fn, 52.38.Kd, 52.59.-f, 52.50.Jm, 42.60.Rn, 42.55.-f, 06.30.Gv

Published in Plasma Phys. Control. Fusion 56 (2014) 084011.

Work supported in part by US Department of Energy under contract DE-AC02-76SF00515.

1. Introduction

The Facility for Advanced Accelerator and Experimental Tests (FACET) at the SLAC National Accelerator Laboratory has operated as a National User Facility since 2011. It supports a broad user program in accelerator science, materials science, and other fields of research. The multi-GeV Plasma Wakefield Acceleration experiments (known as E-200) form the core of the FACET program to demonstrate a single-stage plasma-based accelerator for electrons and positrons. The main goal is to develop a plasma module with beam parameters and energy gain at the level required for novel radiation sources and future linear colliders[1]. Potential applications for plasma wakefield accelerators (PWFA) include Free Electron Laser (FEL) energy doublers and plasma afterburners for a linear collider or a future Higgs factory.

For next generation PWFA experiments, long, uniform, high-density ($> 10^{16}$ e^{-}/cm^{3}) plasmas are required to produce a large energy gain in a single meter-scale module, on the order of tens of GeV. Best performance is achieved when the plasma radius is greater than the blow-out radius, which is on the order of the plasma electron skin depth c/ω_{pe} or about 17μm for the above density. In the SLAC linac, the FACET electron beam is accelerated to 20 GeV with a charge of 3 nC. In E-200 PWFA experiments, a plasma is formed in a heat-pipe oven[2] filled with an alkali metal vapor (Li, Rb or Cs). Lithium is utilized as the plasma source due to its relatively low first ionization potential (5.4 eV) and much higher second electron ionization potential (75.6 eV). As a result, the plasma density reached through ionization is expected to be equal to the lithium atomic vapor density.

In a beam-driven PWFA, head erosion resulting from a finite beam emittance has been shown to be one of the limiting factors in reaching the maximum energy gain[3]. The head of the electron beam is not guided until a plasma is formed; hence a preformed plasma will mitigate the head erosion problem. With a pre-ionized plasma source, energy can be effectively transferred from the electron beam to the wake. In the two-bunch PWFA experiment at FACET[4], a strong drive beam produces an accelerating wake and a second trailing witness beam follows the drive beam at the appropriate distance for acceleration to high energy. With the two-bunch beam parameters at FACET, the drive beam cannot sufficiently ionize the plasma, and even if it could, head erosion would limit the distance over which acceleration can occur. Therefore, a laser ionization scheme using axicon focusing has been developed to turn Li vapor into a preformed meter-scale homogenous plasma[5]. Discussion of the ionization process and the use of the axicon lens are detailed in Ref.[5]. The laser ionized plasma electron density drops by a factor of two in approximately 1.5 ns due to recombination, and thus needs to be synchronized with the arrival of the electron bunch and controlled to ∼100 ps or better.

Single ionization of lithium demands maintaining a laser intensity larger than $\sim 10^{12}$ Watts/cm^2 (based on an analytical estimate of multiphoton ionization[5]) over the desired plasma radius ($\sim$ 1 mm) and length ($\sim$ 1.5 m). The minimum laser energy required depends on the ionization potential, density, and the volume of the vapor to

be ionized. To make a 1.5 m long lithium plasma with a radius of 1 mm and a density of $\sim 5 \times 10^{16}$ e^-/cm^3, the minimum laser energy is about 200 mJ, corresponding to a minimum peak power of 4 TW for a 50-fs (FWHM) laser pulse.

The E-200 experiments are the first to utilize the FACET laser to generate a preformed plasma over 30 cm in length in June and December of 2013. Laser and axicon lens have been used to generate cm-scale plasmas in other experiments[6][7][8]. This paper describes plasma formation with the 10-TW FACET laser system and the setup for the first experiments, in which laser pulses were compressed to 250 fs, injected into a vapor cell, and focused by an axicon lens to form the plasma. The interaction of the 20-GeV FACET electron beam with this preformed plasma leads to acceleration in the wakefield with gradients on the order of a several GeV/m.

2. The Laser System

The 10-TW chirped pulse amplified Ti:Sapphire laser system was conceived, designed, installed and commissioned in less than seven months. The laser system consists of the front end laser, preamplifier, main amplifier, 28-meter-long laser transport line, compressor, and timing system, as described in the following subsections. The 10-TW laser system enhances the FACET experimental program and enables a number of experiments utilizing a high-energy and/or high peak-power laser with the FACET electron or positron beam.

2.1. The Front End Laser System, Preamplifier, and Main Amplifier

The laser oscillator is a Vitara-T from Coherent Inc., which operates at a center wavelength of 800 nm with a spectral bandwidth of 60 nm FWHM and a mode-locking rate of 68 MHz. The oscillator is locked at the 8th harmonic of the 476-MHz radiofrequency (RF) master reference of the SLAC linac, allowing control of the timing of the laser relative to the FACET beam. The oscillator is followed by a commercial regenerative amplifier (Regen) from Coherent Inc (Legend Elite HE USP), where a portion of the laser is extracted prior to the Regen's compressor to seed the amplifiers.

The Regen operates at 120 Hz, the maximum repetition rate of the electron beam in the SLAC Linac, and is triggered by the linac timing system. The Regen output laser repetition rate is divided down to 1 or 10 Hz to match the beam repetition rate delivered to the FACET experimental area. One millijoule of the Regen's uncompressed output energy is used for the power amplifiers designed at SLAC. The first stage is an intermediate 4 pass preamplifier that delivers a 30 mJ seed to the main amplifier. The preamplifier is pumped by a Quantel CFR200 YAG flash lamp laser that can produce 130 mJ of 532 nm light at 10 Hz. It uses an 8 mm diameter, 15 mm long Ti:Sapphire rod that is water cooled.

A 4-pass main amplifier brings the energy up to $\sim$ 1 J using two Thales SAGA YAG flash lamp lasers that each produces 1.8 J of 532 nm light at 10 Hz. In this case,

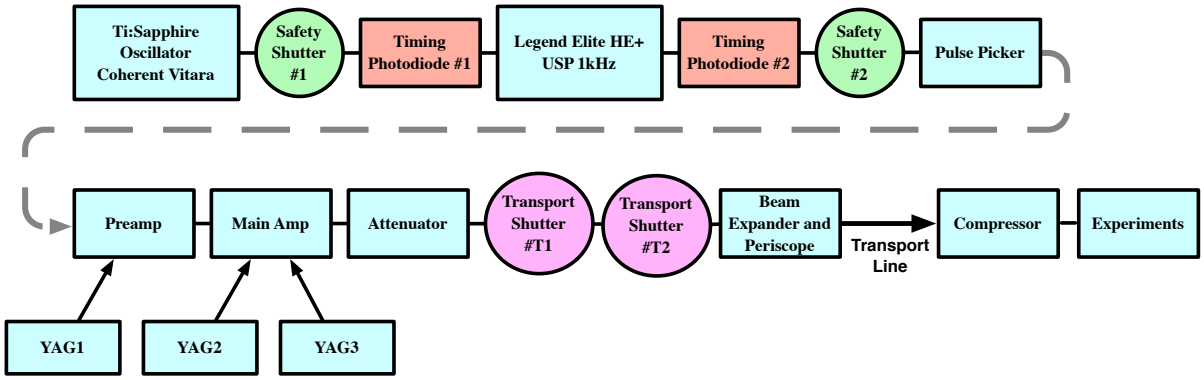

Figure 1: A diagram of the laser system.

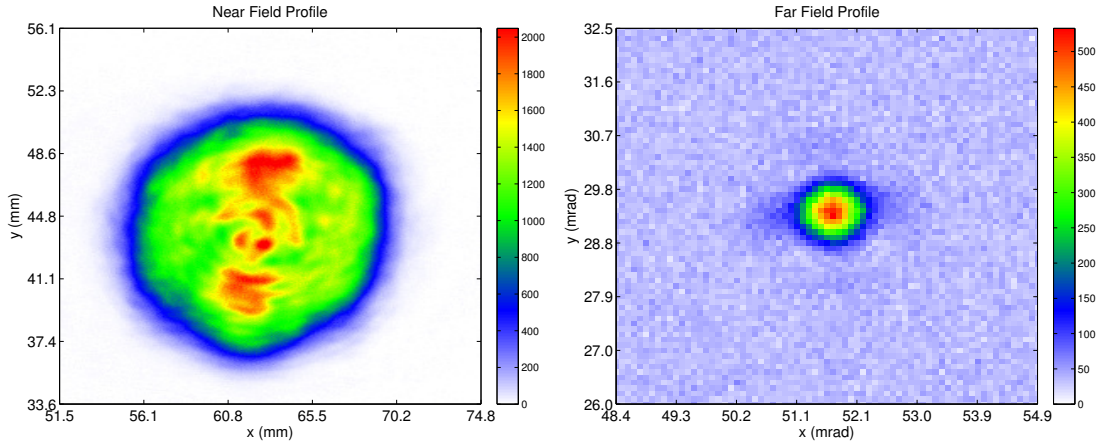

Figure 2: Laser near and far field profiles after the main amplifier. The laser has flat-top profile with $\sim 25\%$ intensity variation.

the Ti:Sapphire crystal is a 20-mm-diameter, 20-mm-long water-cooled rod. The entire laser amplifier system fits onto two optical tables located in the FACET laser room, at ground level next to the Klystron Gallery at Sector 20 of the SLAC Linac (2 km from the start of the 3-km linac), just above the FACET experimental area. The laser system layout is illustrated in Fig. 1.

Two CCD cameras were set up to sample the laser profiles after the main amplifier and before laser is transported out of the laser room. Figure 2 shows images of the near and far field profiles. These cameras are used to assess the laser mode intensity and phase profiles, as well as recover the launch vector into the transport.

2.2. Laser Synchronization to the e-Beam

The laser needs to be synchronized with the FACET e-beam for PWFA experiments. A photodiode is used to time the laser to the electron beam within 1 ns. The photodiode is placed at a location on the beam line where both the laser signal and optical transition radiation from the electron bunch can be detected. The timing of the laser is adjusted to

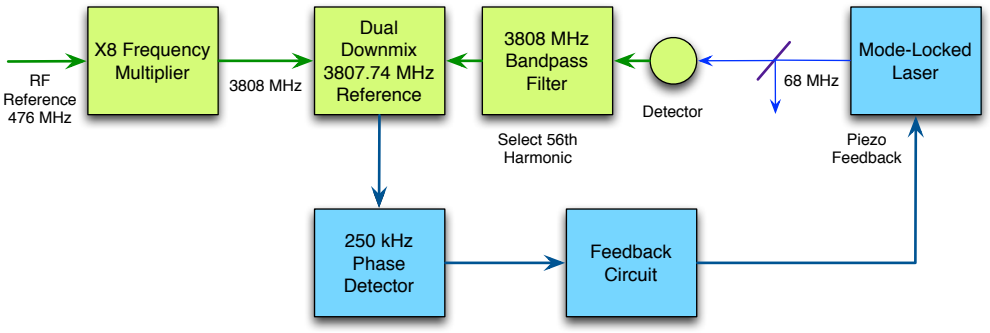

Figure 3: A block diagram for the laser locking system.

place the laser pulse about 1 ns before the arrival of the electron beam. The resolution is limited to 1 ns by the photodiode, long cables, and the oscilloscope. Fine timing to ensure the e-beam arrives before the plasma density decays is done with the plasma acceleration signal itself. The laser timing is stepped in 100 ps increments until there is no evidence of beam-plasma interaction on downstream beam imaging diagnostics, which indicates that the laser pulse arrives after the passage of electron beam. From this point, the laser arrival time is stepped forward in 10 ps increments until it is roughly 100 ps ahead of the e-beam.

The FACET laser is locked by an RF synchronization and phase stabilization system developed at SLAC. The timing system makes use of custom modular components designed to fit into a simple off-the-shelf chassis, thereby enabling flexible controls system requirements. The locking system consists of an RF downmixer, a phase detector, a frequency multiplier, a phase shifter and controller, a feedback unit, and a trigger re-synchronizer, as illustrated in the block diagram of Fig. 3. The RF system locks the 56th harmonic (3808 MHz) of the 68 MHz mode-locked oscillator to the 8th harmonic of the 476 MHz accelerator master reference source. The laser oscillator pulse time relative to triggers is controlled by adjusting the cavity length of the Vitara oscillator via the Phase Shifter to delay the oscillator relative to the accelerator RF system.

The laser jitter with respect to the RF reference has been measured to 70 fs or better in a bandwidth from 10 Hz to 10 kHz. Long-term drift over days has been estimated at < 10 ps. The jitter between the laser and the electron beam is much larger (~ 1 ps) than the jitter of the laser pulse arrival. In the 2 km of SLAC linac used to accelerate and compress the FACET electron bunch, phase and energy jitter result in arrival time variation of the electron beam on the order of < 1 ps. This value is empirically determined by the laser delay needed to transition from no preformed plasma interaction to preformed plasma interaction on every shot. An electro-optic sampling system is currently being commissioned to quantify this jitter on a pulse-to-pulse basis.

2.3. Laser Transport

The laser pulses are transported from the laser room to the FACET experimental area located inside the linac tunnel, 10 m below ground. The transport tubes pass through the wall from the laser lab to the Klystron Gallery, then along and across the Klystron Gallery and down through a penetration to the linac tunnel. To avoid beam quality degradation along the long transport beam line due to the high peak power and thus possible optics damage, the uncompressed laser is transported through a system of five evacuated stainless steel tubes with a diameter of 6 inches (150 mm).

The main amplifier output plane is relay-imaged to the entrance plane of the compressor. There are two imaging stages: the magnification of the first stage is 3:1 and that of the second is 1:1. Each stage of the imaging system produces a focus in the laser transport line. Therefore, it is essential to keep the transport tubes under vacuum to avoid air breakdown at the focal points which would cause laser shape and phase instabilities. The 28-meter-long transport line is evacuated to a vacuum pressure of 10^{-5} Torr. A vacuum also avoids laser pointing instabilities from air convection driven by uncontrolled temperature changes in the Klystron Gallery. The output of the imaging system preserves the collimated input laser qualities.

There are five dielectric turning mirrors in the transport line, and each is controlled remotely to align the laser. To aid the alignment, a network camera is installed behind each of the turning mirrors. Each camera is placed outside the vacuum and allows observation through a viewport of the laser spot on a thin glass diffuser mounted directly behind the dielectric transport mirror.

2.4. Laser Compressor

The laser pulses are compressed using a grating compressor in a vacuum chamber at the end of the transport line. The compressor chamber is adjacent to the FACET beamline, illustrated in Figure 4.

The stretched pulses coming out of the main amplifier have a spectral bandwidth of 24 nm FWHM and can be compressed down to less than 50 fs FWHM. The compressor is a two-grating compressor with a vertical retro-reflector. Because of the high peak power reached after compression (up to 10 TW), the compressor chamber has to be under vacuum. To avoid self-phase modulation when passing through the optics in the Interaction Point (IP) chamber, the compressor (separation of the gratings) is detuned to increase the pulse length to ~ 250 fs. At the output of the chamber, an anti-reflective coated window isolates the vacuum between the compressor and the FACET beam line. The total transmission efficiency of the laser transport line and compressor has been measured to be about 60%.

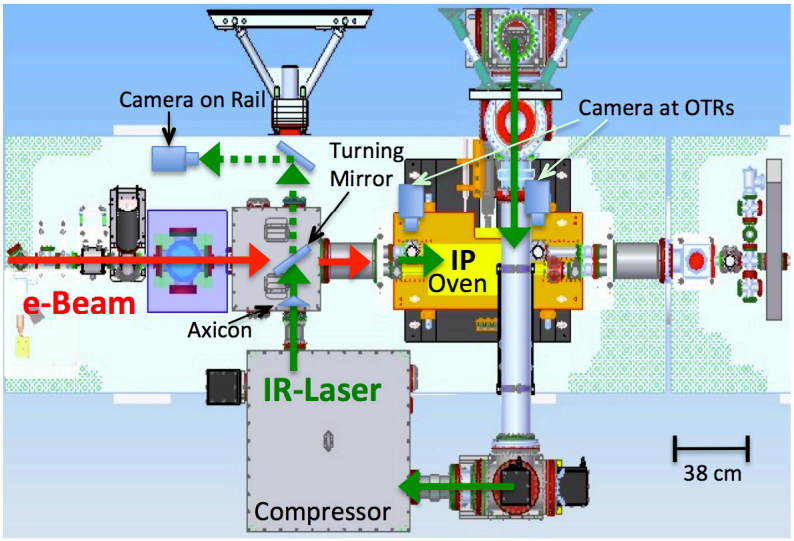

Figure 4: A top view of the laser transported to the experiment. The turning mirror and axicon lens are not drawn to scale. The dashed path is used for laser diagnostics when the turning mirror is extracted to allow the laser pulses to be brought outside of the chamber for equivalent plane imaging.

2.5. Integration of Particle and Laser Beams

The laser pulses leaving the compressor are sent into a chamber in the FACET beam line. Figure 4 shows a top view of the beam path at the location of the PWFA experiment and the two optics inside this chamber. The compressed laser pulses pass through a 2″ (50 mm) diameter, 1.5° fused silica axicon lens with a mask of 3/8″ (9.5 mm) diameter. The turning mirror is gold-plated with BK7 substrate and has a 4-mm diameter central hole to allow passage of the electron beam, thus allowing the laser pulses to travel collinearly with the electron beam.

Laser pulses injected into the vapor cell are focused by the axicon lens to form the plasma. For practical reasons, a conventional spherical lens cannot produce a uniform high-intensity profile over a meter-scale distance but an axicon lens[9] can. The axicon lens also requires lower laser power than the conventional spherical lens. Figure 5 illustrates the laser ray tracing and the focal region where laser ionization leads to plasma formation. After the line focus, the laser diverges and is dumped onto a glass neutral density filter, which protects a beryllium vacuum window located further downstream that is used to isolate experimental vacuum region from the linac vacuum. The pointing stability of the laser focus has been measured to be 37 μrad (RMS) at a location 2.7 m downstream of the axicon lens.

The length of the plasma column depends on the angle of the axicon lens and the diameter of the laser beam. Using an axicon lens with a smaller apex angle increases the plasma length by the ratio of the angles of the lenses. For example, reducing the axicon angle from a 2° to 0.5° lengthens the plasma from 40 cm to 160 cm, but requires

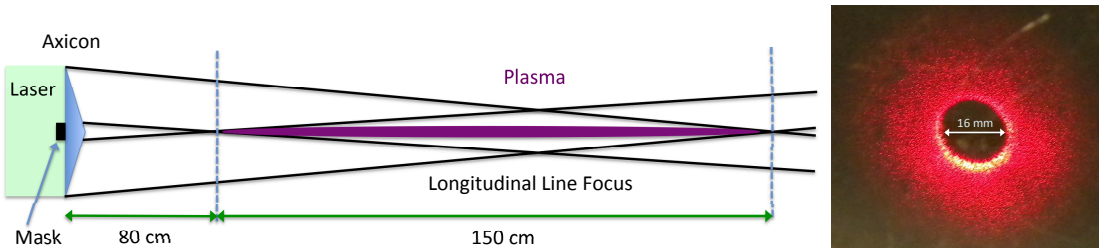

Figure 5: Laser ray tracing (left, not drawn to scale) and picture of laser dump after line focus (right).

proportionally more laser energy to maintain the same peak intensity. The diameter of the laser, which is restricted by the aperture of a mask just in front of the axicon lens, also controls the ionization length since it determines where the focal line ends, as illustrated in Fig. 5. A smaller circular mask centered on the laser axis at the same plane as the outer mask likewise determines where the focal line begins. The mask blocks the central laser rays that define the start of the line focus. The laser energy delivered to the axicon was about 140 mJ for the first experiment in June 2013, and it was about 480 mJ in December 2013 after a laser energy upgrade.

The E-200 experiments also require spatial overlap of the laser and the electron beam. A phosphor screen is mounted on the back of the turning mirror in Fig. 4 to aid in beam positioning. To align the electron beam and the laser along the axis of the oven, a motorized translation stage moves the oven to the side and substitutes a bypass line with two optical transition radiation (OTR) targets at locations roughly corresponding to either end of the plasma. A 500-μm-thick titanium disc generates an OTR signal from the electron beam and also reflects light from the laser; both profiles are measured by a CCD camera at each OTR location. The pointing of the laser is adjusted until the two beams are spatially overlapped to $< 50\mu$m at each OTR target. The laser pulses propagate through the axicon lens and form a Bessel intensity profile when aligned as expected.

3. Results

A laser-ionized plasma column of 36 cm (FWHM) long with a diameter of about 1.2 mm was formed and used for the E-200 PWFA experiments at FACET. A 1.5° axicon lens was used in combination with a 480 mJ, 42 mm diameter laser pulse compressed to 250 fs. The diameter of the plasma column was determined by translating the final turning mirror and hence the laser pulse parallel while observing the accelerated feature of the beam.

The final turning mirror can be extracted to allow the laser pulses to be brought outside of the chamber for equivalent plane imaging. A CCD camera on a rail (Fig. 4) is positioned at the equivalent locations of the entrance and exit of the oven relative to the axicon lens. The transverse laser profiles captured by the camera shown in Fig. 6

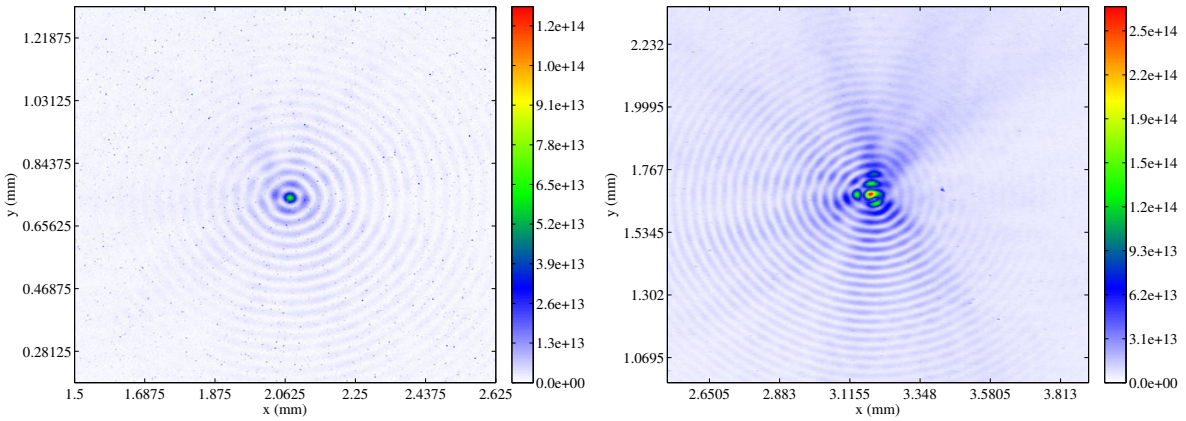

Figure 6: Images of the axicon-focused laser intensity profile: at the entrance of the oven or ∼70 cm from the axicon (left), and the exit of the oven or ∼160 cm from the axicon (right). The color bars indicate laser intensities in unit of W/cm^2 and show that both profiles contain the required intensity $> 10^{12}$ W/cm^2 to singly ionize the lithium vapor.

confirm that a Bessel profile is maintained to the end of the oven. The images in Fig. 6 were taken with an attenuated ∼20 mJ laser and the color bar has been scaled to reflect the projected intensity for the full energy laser which is 480 mJ. More importantly, the laser intensity ($> 10^{12}$ W/cm^2) is high enough to fully ionize Li vapor in the experiments with density of 5×10^{16} e/cm^3.

When the final turning mirror is inserted, another CCD camera captures an image of a laser ionization filament (Fig. 7) through a viewport in the oven bypass line where only argon gas is present. The presence of the filament indicates that the laser is able to ionize argon. The compressed electron beam is also strong enough to ionize argon. When the laser and electron beam are spatially aligned, the two filaments overlap one another.

The latest E-200 experiment observed a clear difference between the interaction of the electron beam in a lithium plasma ionized by the electron beam itself and a plasma generated by the laser[4]. More energy gain and more participating charge were observed when the laser was fired into the lithium vapor ahead of the electron beam. This was a good indication that the electron beam was going through a laser-ionized lithium plasma. In the two-bunch experiments, the witness bunch was accelerated to higher energies in a laser-ionized plasma due to a longer beam-plasma interaction length.

The laser intensity required for ionization of lithium, hydrogen, and argon is $\sim 10^{12}$ W/cm^2, $\sim 10^{14}$ W/cm^2, and $\sim 10^{14}$ W/cm^2, respectively. Since ionizations of argon and lithium were observed, one can expect that hydrogen can also be ionized. This shows that PWFA experiments performed with hydrogen gas are feasible. There is only one electron available to be ionized in hydrogen, and thus experiments can avoid the potential problem of secondary ionization as can be the case with lithium, cesium, or rubidium for example. The ease of bringing hydrogen gas to and from the experimental

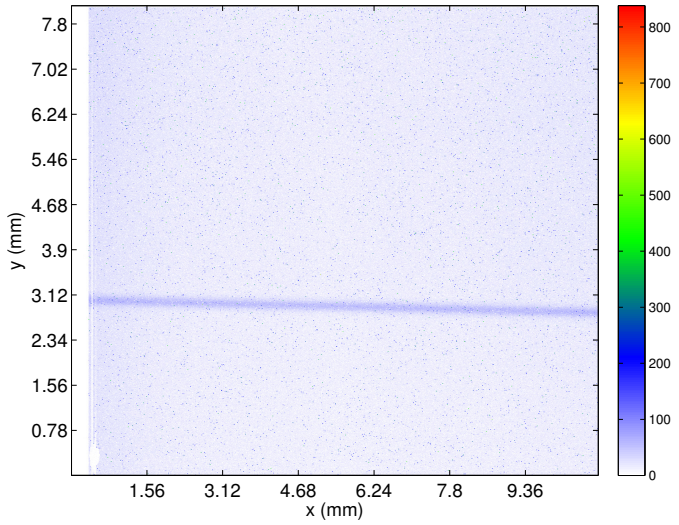

Figure 7: Image of the plasma recombination light taken at the beginning of the axicon focal line shows a laser ionized filament in the argon gas. The color bar indicates the light intensity in arbitrary units.

chamber and lack of residual or mixed waste are some of the added advantages that make it an attractive choice for future PWFA experiments.

4. Conclusion and Outlook

A laser system for the first laser-ionized plasma wakefield acceleration experiments has been successfully commissioned and operated at FACET. The use of an axicon lens was demonstrated to focus a laser that ionizes the lithium alkali metal vapor to form a 36-cm plasma column suitable for PWFA. The E-200 experiments performed at FACET used this technique for plasma formation and achieved high-efficiency acceleration of an electron beam[4]. These experiments used lithium because of its low ionization potential. However, a laser intensity of $> 10^{14}$ W/cm^2 is sufficient to ionize a hydrogen-filled gas cell as well. Therefore, future PWFA experiments may choose to use hydrogen as the plasma source.

Most recently, good quality axicon profiles have been created over a 1.5 m distance. In the next E-200 experimental run, the 40 cm long Li oven will be replaced with one of 1.5 m in length. A smaller angle axicon lens will be used for plasma formation over the increased length. The expectation is that these changes to the FACET PWFA experiments will result in energy gains in excess of 10 GeV.

The pre-ionization for PWFA presented in this paper is an example of just one experimental application of the 10-TW laser system. Other applications of high power lasers with electron beams include Thomson backscatter for bright directional gamma-ray production[10], imaging of the evolving beam-driven plasma structures[11], and Faraday rotation diagnostics of the accelerating beam inside the PWFA[12], as well

as applications of synchronized auxiliary laser pulses that have been demonstrated in connection with laser-driven wakes.

In summary, the high power laser opens up numerous exciting possisbilities for new experiments at FACET. One example is the Trojan Horse Plasma Wakefield Acceleration [13] where electrons are released in plasma wave with a focused, ∼50 fs, ∼1 mJ, synchronized laser pulse to generate a high brightness witness beam ($\epsilon_n < 10^{-8}$ m-rad). Another experiment being tested at FACET is the self-modulation of long lepton bunches ($\sigma_z \sim 500\mu m$) in a dense laser-ionized plasma ($n_e = 0.6 - 2.3 \times 10^{17}/cm^3$)[14]. Experiments without plasma including the optical probe[15] and terahertz radiation pump-probe measurements[16] can be performed by utilizing both the high-field terahertz pulses from the electron beam and the laser at FACET.

Acknowledgments

The authors would like to thank the SLAC Test Facilities Department, the Controls Department, the Mechanical Fabrication Department, the Sector 0-20 and Accelerator Operations and Safety Divisions, and the LCLS Laser Science & Technology Division for their efforts and support in building the FACET laser system. This work is supported by the U.S. Department of Energy under contract numbers DE-AC02-76SF00515 and FG02-92-ER40727.

References

[1] E. Adli et al., "A Beam Driven Plasma-Wakefield Linear Collider: From Higgs Factory to Multi-TeV", arXiv:1308.1145 [physics.acc-ph] (2013).

[2] P. Muggli et al., "Photo-ionized Lithium Source for Plasma Accelerator Applications", IEEE Trans. Plasma Sci. 27, 791-799 (1999).

[3] I. Blumenfeld et al., "Energy Doubling of 42 GeV Electrons in a Metre Scale Plasma Wakefield Accelerator", Nature 445, 741-744 (2007).

[4] M. Litos et al., "High Efficiency Acceleration of an Electron Beam in a High Gradient Plasma Wakefield Accelerator", submitted.

[5] N. Vafaei-Najafabadi et al., "Meter scale plasma source for plasma wakefield experiments", AIP Conference Proceedings, 1507, 650-655 (2012), DOI:http://dx.doi.org/10.1063/1.4773774.

[6] I. Alexeev et al. "Measurement of the Superluminal Group Velocity of an Ultrashort Bessel Beam Pulse", Phys. Rev. Lett. 88, 073901 (2002).

[7] S.J. Yoon, et al. "Quasi-Phase-Matched Acceleration of Electrons in a Corrugated Plasma Channel", Phys. Rev. ST Accel. Beams 15, 081305 (2012).

[8] J. Fan et al. "Tubular Plasma Generation with a High-Power Hollow Bessel Beam", Phys. Rev. E 62, R7603(R) (2000).

[9] J.H. McLeod, "Axicons and Their Uses", J. Opt. Soc. Am., 50, 166 (1960).

[10] S. Chen, et al., "MeV-Energy X Rays from Inverse Compton Scattering with Laser-Wakefield Accelerated Electrons", Phys. Rev. Lett. 110, 155003 (2013).

[11] Z. Li et al. "Single-shot Visualization of Evolving, Light-Speed Structures by Multiobject-Plane Phase-Contrast Imaging", Opt. Lett. 38, 5157 (2013).

[12] A. Buck et al., "Real-Time Observation of Laser-Driven Electron Acceleration", Nature Phys. 7, 543 (2011).

[13] B. Hidding et al., "Beyond Injection: Trojan Horse Underdense Photocathode Plasma Wakefield Acceleration", Advanced Accelerator Concepts: 15th Advanced Accelerator Concepts Workshop. Vol. 1507. No. 1. AIP Publishing, 2012.

[14] P. Muggli et al., "Self-modulation of Long Particle Bunches in Plasmas at SLAC", Proceedings of the International Particle Accelerator Conference (IPAC 2012), 2831 2012.

[15] S. de Jong et al., "Speed limit of the insulator-metal transition in magnetite", Nature Materials 12, 882886 (2013).

[16] M. Liu et al., "Terahertz-field-induced insulator-to-metal transition in vanadium dioxide metamaterial", Nature 487:7407, 345-8 (2012).